Arch Biol Sci. 2016;68(2):375-383 DOI:10.2298/ABS150706029L

INITIAL EVENTS IN THE BREAKTHROUGH OF THE EPITHELIAL BARRIER OF THE SMALL INTESTINE BY *ANGIOSTRONGYLUS CANTONENSIS*

Ying Long[1,2], Xuri Zhang[1,2], Binbin Cao[1,2], Liang Yu[1,2], Meks Tukayo [1,2], Chonglv Feng[1,2], Yinan Wang[3], Wenzhen Fang[1] and Damin Luo[1,2,*]

[1] *School of Life Sciences, Xiamen University, Xiamen*, Fujian, 361102, China

[2] *State Key Laboratory of Cellular Stress Biology, Xiamen University, Xiamen*, Fujian, 361102, China

[3] *Medical College, Xiamen University, Xiamen*, Fujian, 361102, China

***Corresponding author:** dmluo@xmu.edu.cn

Received: July 6, 2015; **Revised**: October 5, 2015; **Accepted**: October 29, 2015; **Published online**: March 23, 2016

Abstract: Although the third-stage larvae of *Angiostrongylus cantonensis* (AcL3) are thought to initiate infection by penetrating the epithelium of the small intestine, the mode of intestinal invasion remains obscure. Considering the inaccessibility of the gut tract and the need to sacrifice animals for this type of study, we devised an *in vitro* cell-parasite co-culture system to examine the initial cellular and molecular events between AcL3 and host epithelia. No apoptosis augmentation was detected in enterocytes after introduction of larvae. A significant increase in dead cells was detected in IEC-6, NCM460 and 293T after incubating for 4 h, with AcL3 wounding rat small intestinal epithelial cells IEC-6 more rapidly. Under a scanning electron microscope (SEM), cell gap opening was visualized in the IEC-6 monolayer treated with AcL3. Loosening of the extracellular matrix (ECM) of the monolayer was found to be involved in the parasite-cell interactions. Pretreating the AcL3 with a protease inhibitor attenuated its penetration ability of the artificial intestine barrier. In conclusion, AcL3 broke through the intestinal barrier of the host with the assistance of mechanical injury and the opening of a cell gap, but without causing apoptosis. The interaction platform presented here may provide direct insight into the cellular and molecular events during worm invasion of host enterocytes.

Key words: *Angiostrongylus cantonensis*; intestinal penetration; apoptosis; mechanical injury; ECM degradation

INTRODUCTION

Angiostrongylus cantonensis is the primary pathogen of human eosinophilic meningitis by accidental infection [1]. As of 2008, over 2800 individuals have been reported to suffer from *A. cantonensis* infection [2]. Recently, the global spread of this disease from traditional areas to more than 30 countries [3], and especially several outbreaks [4-6], has attracted considerable attention.

Rats and non-permissive hosts acquire the third-stage larvae of *A. cantonensis* (AcL3) by consuming infected snails or transport hosts [7,8]. When the AcL3 infective larvae are swallowed and eventually reach the small intestine, they penetrate through the epithelium into the systemic circulation. The intestinal epithelium is acts as a barrier that AcL3 must overcome to infect hosts. Although apoptosis-inducing and cell-gap widening are thought to be involved in the parasitic invasion of tissue [9,10], and various proteases have been shown to have a predicted function during the parasite invasion of host [11-16], there is no detailed molecular pattern of penetration. The excellent work of Lee et al. points out that the serine protease and metalloprotease in excretion-secretion products (ESPs) of AcL3 give assistance in the host gut penetration [17]. Even so, considering the inaccessibility of the gut tract and the need to sacrifice live animals, a new method and more data are needed.

The initial interaction occurs between the nematodes and the intestinal epithelium once AcL3 enters

the host via ingestion. In this work, we describe a cell-parasite co-culture system to observe this initial interaction *in vitro*. We used different types of cell lines to check the tissue-specificity of interaction. The aim of the present work was to see whether ECM loosening occurs and assists in the infection with the worm, or whether the buccal stylet of the AcL3 [18] assists in the penetration by causing mechanical injury, eliciting death of the enterocyte. We hope that this interaction platform can be used to evaluate the tissue or molecular events that occurred during the worm's invasion of the intestinal epithelium.

MATERIALS AND METHODS

Ethics statement

Sprague Dawley (SD) rats were managed and housed in the Xiamen University Laboratory Animal Center, and were allowed food and water *ad libitum*. This study was performed in strict adherence to the Regulations for the Administration of Affairs Concerning Experimental Animals (as approved by the State Council of the People's Republic of China). The protocol was approved by the Committee for the Care and Ethics of Laboratory Animals of Xiamen University (Permit Number: XMULAC2012-0122).

Nematodes

The *A. cantonensis* strain was maintained in SD rats and snails, and the AcL3s were collected as previously described [12]. The sugar flotation technique was used to collect the first-stage larvae of *A. cantonensis* from infected SD rat feces after the 45th day. Fresh positive rat feces, to which water was added to form a paste, were applied to the surface of lettuce. Apple snails (*Pomacea canaliculata*) were then fed on a diet of this lettuce and were consequently infected. After 3 weeks of being infected, the snails were cut into small pieces and digested overnight in digestive fluid (0.7% pepsin in 0.5% HCl). The AcL3s were collected under a dissecting microscope and used in subsequent experiments.

Cell culture

A rat small intestinal epithelial and a human renal cell lines, IEC-6 (CRL-1592) and 293T (CRL-11268), respectively, were obtained from the American Type Culture Collection (ATCC, Rockville, MD). The 293T cell line was chosen because it is an epithelial cell line that is derived from the non-digestive system. These two cell lines were cultured following the recommendation of the ATCC. The NCM460 cell line (INCELL Corporation, LLC), a human colon epithelial cell line, was a gift from Prof. Tianhui Hu of the medical college of Xiamen University, and the cell line was cultured as described in the manual.

The co-culture system

The co-culture system was based on permeable supports. The bottom chamber was the well of a cell culture plate in which the insert, a support coupled with a filter at the bottom, was assembled to avoid direct contact between the AcL3s and cells. Larvae were added to the upper or bottom chambers according to the different needs of the assay.

Apoptosis assay

Epithelial cells were cultured in 24-well plates to 80% confluence as described above. The upper chamber was coupled with a 0.45-μm filter membrane, which allowed molecular interaction while excluding larvae from the bottom chamber, and then 1000 AcL3s were pipetted into the upper chamber (Fig. 1A). Groups of cells treated with 1 μM of etoposide and the same volume of Dulbecco's modified eagle medium (DMEM) served as positive and negative controls, respectively. After 6 h in the incubator, the monolayer cells were rinsed and fixed. All treated cells were analyzed under a fluorescent microscope, and a rabbit anti-cleaved caspase-3 (Asp175) antibody (Cell Signaling Technology), considered a marker of apoptosis, was used to label the apoptotic cells. Three visual field tests were randomLy selected and calculated in each of the triplicate trials.

Worm wound assay

The worm wound assay was performed as previously described with some modifications [19]. Cells were cultured in 48-well cell culture plates overnight to 90% confluence. Fifty AcL3s were suspended in 0.5 mL of medium without serum plus 1.75% agarose, and the mixture was then overlaid on the epithelial monolayer. The same volume of agarose medium without worms served as a control. After incubating for 0, 2 and 4 h, the monolayers were then rinsed and stained with trypan blue dye according to the protocol described by Perry [20]. The stained cells in each well were analyzed and counted under a light microscope for statistical analysis after background correction.

ECM degradation assay

The cells were cultured on a glass coverslip in the wells of a 24-well plate. When it achieved 90% confluence, the medium without serum was applied, a top chamber as described in the apoptosis assay section was assembled and two groups of AcL3s that were treated or not treated with inhibitors were introduced. In addition, the same volume of ESPs from the larvae was collected to investigate their impact on the ECM of IEC-6. After incubating under standard cell culture conditions, the coverslip was removed for immunofluorescence staining or scanning electron microscope (SEM) analysis. The working concentrations in the inhibitor cocktail were 10 mM of aprotinin, 1 M EDTA, 100 mM E64 and 10 mg/mL of pepstatin diluted in DMEM. All commercial inhibitors were purchased from ApexBio (Boston, MA).

Invasion assay

One hundred AcL3s were incubated in 100 μL of inhibitor cocktail or each single inhibitor for 30 min and then introduced into the upper chamber with a Matrigel-coated filter and a monolayer of IEC-6 at 90% confluence in serum-free medium (Fig. 1B). Unlike the filter used above, the one in this assay allowed the worms to penetrate into the bottom chamber (Fig. 1C). The apparatus was placed in an incubator with a

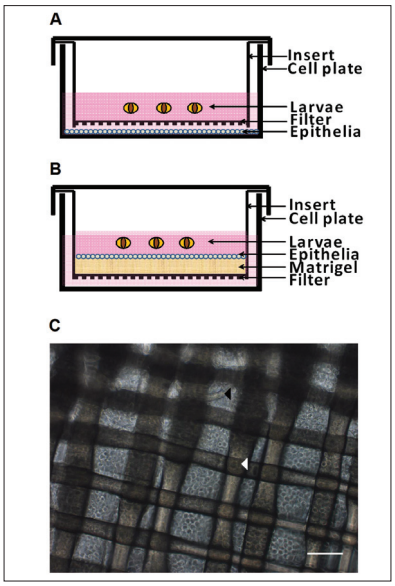

Fig. 1. Schematic diagrams of the parasite-cell co-culture system. **A.** The bottom chamber in the co-culture equipment was a well in the cell culture plate where the insert, a support coupled with a 0.45-μm filter membrane at the bottom, was assembled to allow interactions between AcL3s and cells, while avoiding direct contact. The larvae were added to the upper or bottom chambers according to the different needs of the assay. **B.** As for the invasion assay, a filter membrane that allowed AcL3 to pass through was coated with Matrigel for an enterocyte attachment at the bottom of the insert, mimicking the intestinal barrier; AcL3s were then injected into the upper chamber. **C.** The system for the invasion assay was visualized under an inverted microscopy. Black triangle – AcL3; white triangle – filter; bar=100 μm.

gas phase of 5% CO_2 for 3 h at 37°C. The number of AcL3s that penetrated through the artificial barrier and entered into the bottom chamber was counted after incubating under an inverted microscope. The viability of the worms remaining in the upper chamber was also assessed by microscopy. The penetration ability of the larvae was investigated, and the control group was 100 AcL3s in 100 μL of DMEM without any inhibitors.

Immunofluorescence staining

Immunofluorescence (IF) staining was performed as described previously [21]. In brief, the treated cells were rinsed with precooled phosphate-buffered saline (PBS, pH 7.4) and fixed. The cells were soaked in

0.25% Triton X-100 solution in PBS for 15 min so they would permeabilize. Incubation with primary and secondary antibodies was subsequently performed after blocking. Primary antibodies against cleaved caspase-3 (1:400) and laminin (Sigma-Aldrich, 1:100) were used according to the recommendations in the manual. DAPI (Sigma-Aldrich) was used to color the nucleus with a 5-min incubation in the dark. Stained cells were analyzed with a fluorescence microscope and the images were captured by a digital camera and Image-Pro Plus (version 6.0) software.

Scanning electron microscopy (SEM)

The method used to prepare the specimen for SEM was based on the procedure described by Fuller et al. [22]. A treated coverslip was fixed in 2.5% glutaraldehyde for 2 h at room temperature followed by three rinses with PB (0.1 M, pH7.4). Dehydration was performed through a graded series of ethanol washes. After drying under CO_2, the specimens were coated with gold. Visualization was performed using a LEO 1530 SEM.

Statistics

All the assays were carried out in triplicate at least and the values expressed as the means±standard deviation (SD). Significant differences between groups were analyzed by t-test or one-way analysis of variance (ANOVA) followed by Duncan's multiple comparison test with SPSS 13.0 (SPSS, Inc., Chicago, IL, USA), with a P value <0.05 considered statistically significant.

RESULTS

The ESPs ofAcL3 did not induce IEC-6 apoptosis

As shown in Fig. 2A, the apoptotic cells in the IEC-6 monolayer displayed a positive signal with green fluorescence, under the fluorescence microscope. After 6 h of incubation with AcL3, the number of positive cells in the larvae-treated groups did not differ significantly from that of the control (P=0.8278, P>0.05) (Fig. 2B). Furthermore, we detected the level of apoptosis in NCM460s that were exposed to AcL3 (Fig. 3). All treated monolayer cells exhibited an equal level of apoptosis in comparison with the control, suggesting that apoptosis was not induced by larvae that had been co-cultured with these epithelial cells.

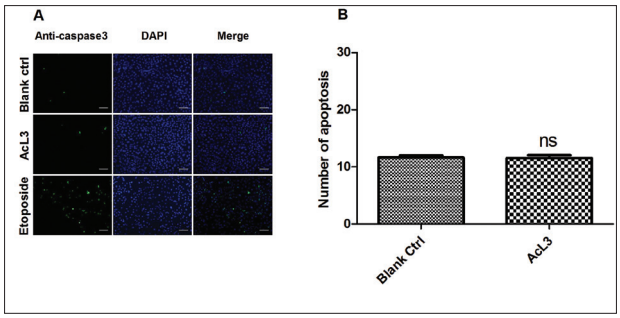

Fig. 2. Apoptosis assay of IEC-6 after incubation with AcL3. **A.** IEC-6 cells were grown to confluence in the bottom chamber for the apoptosis assay. After 6 h of incubation with AcL3, the apoptotic cells were labeled with an antibody against activated caspase-3 (green); the nucleus was stained with DAPI (blue). The blank consisted of IEC-6s without AcL3. After merging the images, the number of positive cells was counted. Ten μM of etoposide was used to induce apoptosis, and served as the positive control. **B.** Results shown as the means±SD from three independent experiments. No significant difference between the two groups were found by the t- test; ns – not significant; bar=100 μm.

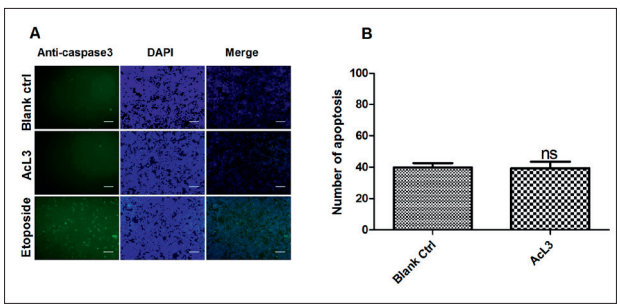

Fig. 3. Apoptosis assay of NCM460 after incubation with AcL3. **A.** NCM460 cells were grown to confluence in the bottom chamber for the apoptosis assay. After 6 h of incubation with AcL3, apoptotic cells were labeled with an antibody against activated caspase-3 (green); the nucleus was stained with DAPI (blue). The blank was NCM460 without AcL3. After the images were merged, the number of positive cells was counted. Ten μM of etoposide was used to induce apoptosis and served as the positive control. **B.** Results shown as the means±SD from three independent experiments. No significant difference between two groups were found by the t-test; ns – not significant; bar=100 μm.

The AcL3s that browsed the epithelial cells wounded them with cell specificity

Pepsin-activated AcL3s were co-cultured with three cell lines in semisolid medium to mimic the *in vivo* condition. The dead cells, in which the membrane was damaged, were dyed blue with trypan blue and viable cells were excluded from staining. Light microscopy studies showed that the larvae that were browsing the monolayer formed by the IEC-6 cell line caused the number of cell deaths to increase significantly (P=6.84×10^{-17}, P<0.05 by ANOVA) after the agar overlay was applied 2 h later (P=1.29×10^{-14}) and 4 h (P=1.68×10^{-17}), in comparison with the control (Fig. 4A, B). However, the number of dead cells did not show a significant increase in the NCM460 (P=0.98, P>0.05) or 293T (P=0.99, P>0.05) after 2 h of incubation, but rapidly reached the same level as that of the IEC-6 after 4 h of incubation relative to the control (P=2.05×10^{-19}, P<0.05 for NCM460; P=8.19×10^{-15}, P<0.05 for 293T). The differential wound caused by AcL3 suggests that the nematodes sensed the host tissues at different time points.

Proteases in the ESPs of AcL3s degraded the epithelial ECM

All treated cells were visualized by SEM to observe the superficial changes in monolayer integrity. Monolayers treated with 1000 AcL3s for 3 h revealed distinct gaps that widened at cell-cell contacts in comparison with the control (Fig. 5B, E), indicating that the ESPs of larvae were essential for this trace, even if the worms did not need to be at the point of contact between neighboring cells. In addition, a protease inhibitor cocktail that was applied to the AcL3 was able to partly attenuate these changes, implying the involvement of proteases in this process.

To quantify the remarkable variation in the monolayers caused by AcL3, the ECM and the cells were labeled with green fluorescence (Fig. 6A). Under the fluorescent microscope, three visual field tests were randomly selected in each of the separate triplicate samples and intercellular gap areas were measured.

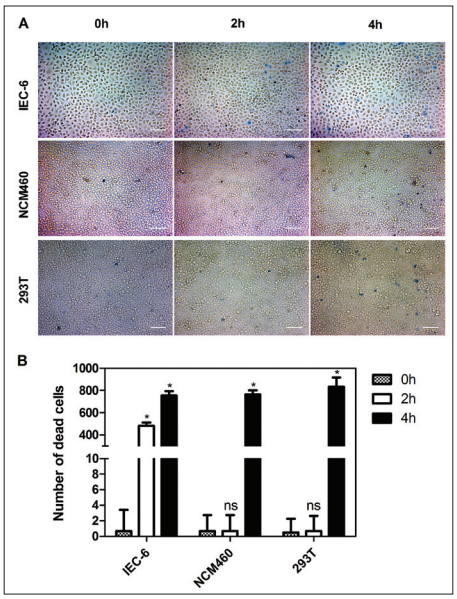

Fig. 4. A wound assay of epithelial monolayers after exposure to AcL3s in a time gradient. **A** Three epithelial cell lines were grown to confluence. AcL3s suspended in agarose plus medium were overlaid on the monolayer. After incubating over a time gradient, the cells were stained with trypan blue to detect the dead cells (blue). **B.** After 4 h, the dead cells had clearly increased in all 3 cell lines. At 2 h, the increase was only detected in the IEC-6 monolayer. The results are presented as the means±SD from six independent experiments. The difference between the means from samples at different time gradients was estimated by one way ANOVA followed by Duncan's multiple comparison test. Asterisk – P<0.05; ns – not significant; bar=100 μm.

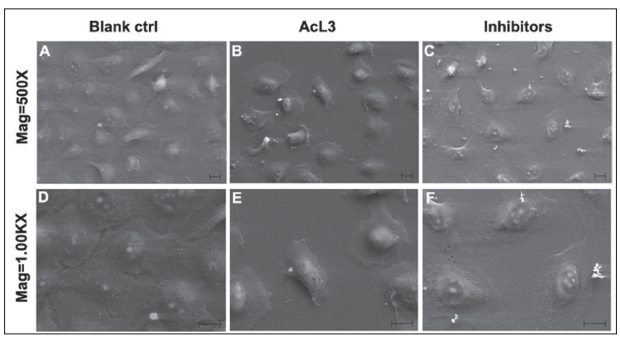

Fig. 5. SEM observation of the superficial change in the IEC-6 monolayer after the introduction of AcL3. IEC-6 cells were grown to confluence on microscope cover slips. AcL3s pretreated with inhibitors (C, F) and normal AcL3s (B, E) were applied to the cells for 3 h. The blank is comprised of IEC-6s without AcL3 (A, D). The cells in the blank group exhibited intact and continuous cell sheets. After treating with AcL3, the cell sheet became cracked (B, E), with obvious gaps present at the cell borders. Inhibitor pretreatment partly attenuated this variation (C, F). Bar=10 μm.

As shown in Fig. 6, all treatments were found to differ significantly by ANOVA (P=2.2×10^{-11}), and Duncan's multiple comparisons further showed the differences among them (P<0.05), i.e., both AcL3 and the ESPs had a considerable effect on the intercellular space in IEC-6 after incubation. In comparison with the blank control, the ESPs (P=2.10×10^{-9}, P<0.05) and AcL3s (P=2.89×10^{-12}, P<0.05) led to 3.08- and 4.47-fold increases in the area value of the intercellular space, respectively. Groups of larvae that had been pretreated with inhibitors also displayed a 1.64-fold increase in comparison with the blank; the remarkable decline in the AcL3 and ESP groups (Fig. 6B) pointed to the alleviative effect of the inhibitor mixture on the cell gap opening. Thus, proteases from AcL3 were observed to be a powerful biochemical weapon in assisting larval penetration of the epithelial barrier.

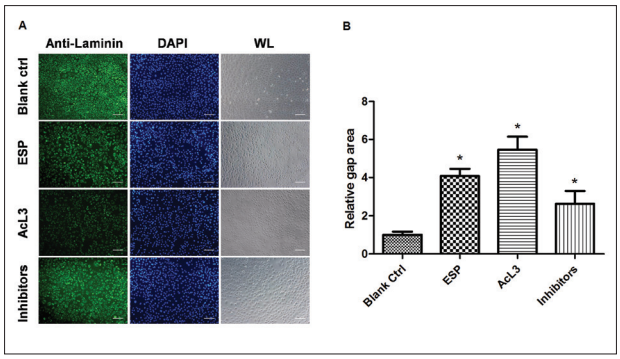

Fig. 6. Quantitative analysis of ECM degradation of IEC-6 after incubation with AcL3. **A.** IEC-6 cells were grown to confluence. AcL3s pretreated with inhibitors and normal AcL3s were applied to the cells for 6 h. The blank was comprised of IEC-6s without AcL3; a comparable amount of ESPs was collected to apply to the ESP group. After incubation, the cytoplasm and ECM were labeled with anti-laminin antiserum (green); the nucleus was stained with DAPI (blue). After the images were merged, the dark area represented the intercellular gap. **B.** The dark area was measured and analyzed. The results are shown as the means±SD from six independent experiments. The difference between the means from each group of samples was estimated using one-way ANOVA followed by Duncan's multiple comparison test. Asterisk – P<0.05; WL – white light; bar=100 μm.

Protease inhibitors blocked worm penetration of the *in vitro* barrier

The invasion of the *in vitro* barrier was observed in AcL3s pretreated with the protease inhibitor mixture, each single inhibitor and the control. A permeable support, which was coated with Matrigel on which cells could be seeded, was used for the *in vitro* invasion assay of infectious larvae (Fig. 1B, C). After 3-h incubation, almost all the larvae were able to pass through the monolayer, gel pad, filter and finally into the bottom chamber. However, preincubating AcL3 with inhibitors led to significant effects on its barrier penetration ability (Fig. 7) according to ANOVA (P=2.2×10^{-11}), and Duncan's multiple comparisons further showed that all treatments differed significantly from the control (P<0.05), i.e., aprotinin, EDTA, E64 and pepstatin effectively blocked 24.7%, 31.0%, 23.5% and 11.5% of the penetration, respectively, indicating an involvement in all four classes of proteases, aspartic protease, metalloprotease, cysteine protease and serine protease, during this process. An inhibitor cocktail prevented 66% of the AcL3 from penetrating the *in vitro* imitative barrier in six separate trials on average. The larvae in the top chamber were visualized by microscopy and no inhibitor influence on parasitic viability was detected after the incubation. Clearly, the

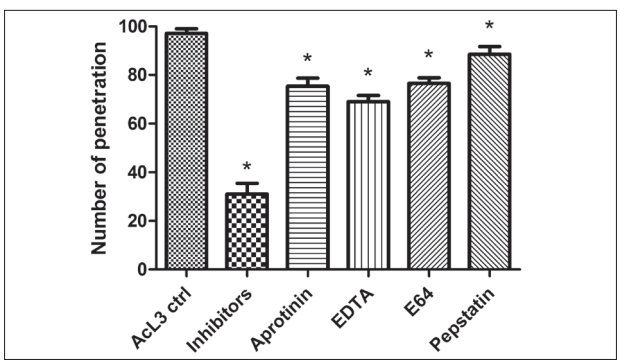

Fig. 7. Protease inhibitors reduced larval penetration of the *in vitro* barrier. IEC-6 cells were grown to confluence on the Matrigel-coated permeable filter. The same number of AcL3s that was pretreated with or without inhibitor cocktail was introduced into the upper chamber for the invasion assay. The effect of a single inhibitor was investigated. The number of AcL3s that penetrated through the barrier was measured. After 3 h of incubation, almost all the larvae passed through the barrier; a 66% decrease was detected in the inhibitor mixture-treated group. Aprotinin, EDTA, E64 and pepstatin were found to block 24.7%, 31.0%, 23.5% and 11.5% of the penetration effectively, respectively. The results are shown as the means±SD from six independent experiments. The difference between samples was estimated by the t-test. Asterisk – p<0.05.

inhibition of protease from AcL3s arrested the invasion of the larvae, implying the essential roles of proteases in breaking through the intestinal epithelium.

DISCUSSION

As in most foodborne pathogens, the small intestine is the site through which they enter the body of a host, and *A. cantonensis* is no exception. Although some *in vivo* studies on the invasion and behaviors of *A. cantonensis* have been established, a detailed investigation of this process has been hindered by obstacles to accessing and manipulating the intestinal environment of the worms. Therefore, we first focused on developing an *in vitro* system that could be used to test the initial interaction between larvae and epithelial cells. Thereafter, the apoptosis assay and other experiments were used to evaluate the initial interaction between AcL3 and epithelial cells *in vitro*. Therefore, the experimental platform presented in this study was feasible and the system might be applied to work as distinctive analyses with a corresponding setup.

Infectious parasites, such as blood fluke and malaria, were documented to induce apoptosis of the host epithelia from the skin and brain, respectively [9,23]. Hu et al. [10] demonstrated that *A. cantonensis* larval extracts had pro-apoptotic effects on both brain microvascular endothelial cells and brain astrocytic cells. Even so, when the influence of mechanical injury to cells was excluded in the apoptosis assay, no apoptosis was induced by ESPs of AcL3, suggesting differential responses of different host cells to the pathogen.

As shown, the worms were allowed to browse the monolayer and were provided a chance to attack the cells after direct injection into the cell plate. Although there seems to be no specificity in the dead cells from all three epithelial monolayers provided with a sufficiently long incubation time, the different cell lines may have distinctive responses to the AcL3 moving over them at different time points. We speculate that AcL3 achieves gut penetration after the essential identification of host enterocytes, despite a lack of clarity regarding the precise mechanism. The small intestinal epithelium was mechanically wounded by AcL3 more rapidly than kidney and colon cells, and this immediate response was likely related to the normal route established between AcL3 and host enterocytes, which represent the first line of host defense. Unlike the large area of enterocyte damage caused by *Trichinella spiralis* [19,24], an augmentation in dotted dead cells was detected in our work. Many cases of trichinellosis present pathological changes in gastrointestinal symptoms, caused by the worm burrowing into the intestine and migrating within it [25,26]; however, no such case was reported during AcL3 invasion of the small intestine [2,27]. Perhaps they had different infection strategies. In one case of abdominal angiostrongyliasis, which was commonly attributed to *A. costaricensis* infection [28], this disease could have been caused by *A. cantonensis*, with eosinophilic accumulation in the mucosa of serosal layers of host sigmoid colon [29]. However, unlike the fact that *A. costaricensis* lived inside intestinal small vessels, *A. cantonensis* had no direct contact with the colon in its life cycle. These symptoms of eosinophilic infiltration in the colon might be related to host interleukin and eosinophil responses [30,31], but not to larval invasion.

Although secreted proteases of AcL3 were indirectly shown to facilitate the host gut breakthrough [17], our results of SEM provide direct evidence that the ESPs of AcL3 opened the epithelial cell sheet of IEC-6. By measuring the dark area representing the gaps, a widening gap between the neighboring cells was observed after treating with AcL3. In addition, cells treated only with a comparable amount of ESPs resulted in less cell-gap widening than that of AcL3, pointing to possible upregulation of some AcL3 genes, which contributed to space broadening. The role of proteolytic enzymes that may be involved in ECM degradation was evaluated by using an inhibitor-based approach.

Lee and Yen [17] developed an entire duodenum model to observe the larval penetration of the gut wall and a 4-h incubation was required for the assay. After only 3-h incubation, the penetration rate of 97% can be measured easily by counting the number of AcL3 in the bottom chamber using the artificial barrier, re-

vealing that this was a time-saving and easy-operating method of assessing the influence of proteases on larval invasion. Unlike the findings of Lee and Yen, our data showed that cysteine protease also functioned in gut penetration of AcL3. Cathepsin B-like cysteine protease was reported to be one of the most abundant transcripts in AcL3 [16] and was documented to play a vital role in the gut penetration of *Fasciola hepatica* [14], which indirectly supported our results. Besides, the cocktail partially blocked larval penetration of the barrier at a rate of 66%, suggesting the involvement of other factors in this process, as for exaple mechanical injury or the involvement of a pore-forming molecule, as previously reported in whipworm [32].

CONCLUSIONS

We established an *in vitro* co-culture model and constructed a platform that was fitted for exploring the precise mechanical changes experienced by host cells during *A. cantonensis* infection. Although details of the mechanism remain to be determined, the present work demonstrates that the ESPs of AcL3 were capable of expanding the cell gaps of the epithelial sheets, and wounding the epithelia derived from the small intestine because by mechanical damage, while apoptotic effects were undetected. The proteases contained in the ESPs played vital roles in hydrolyzing the components of the ECM. We hypothesize that AcL3, after recognizing the intestinal cells, wounded the epithelia and broadened the cell gap by loosening the ECM in order to pass through the barrier.

Acknowledgments: We are grateful to Prof. Tianhui Hu for providing the NCM460 cell line. This work was supported by the National Nature Science Foundation of China (Grant No. 81171595).

Authors' contributions: YL and DL conceived and designed the experiments. YL XZ BC YL and MT performed the experiments. YL and DL analyzed the data. DL YW and WF contributed the reagents/materials/analysis tools. Yl and DL wrote the paper.

Conflict of interest disclosure: The authors have no conflict of interest related to this work.

REFERENCES

1. Alicata JE. Biology and distribution of the rat lungworm, *Angiostrongylus cantonensis*, and its relationship to eosinophilic meningoencephalitis and other neurological disorders of man and animals. Adv Parasitol. 1965;3:223-48.
2. Wang QP, Lai DH, Zhu XQ, Chen XG, Lun ZR. Human angiostrongyliasis. Lancet Infect Dis. 2008;8(10):621-30.
3. Sawanyawisuth K, Chotmongkol V. Eosinophilic meningitis. Handb Clin Neurol. 2013;114:207-15.
4. Wang J, Qi H, Diao Z, Zheng X, Li X, Ma S, Ji A, Yin C. An outbreak of angiostrongyliasis cantonensis in Beijing. J Parasitol. 2010;96(2):377-81.
5. Lv S, Zhang Y, Chen SR, Wang LB, Fang W, Chen F, Jiang JY, Li YL, Du ZW, Zhou XN. Human angiostrongyliasis outbreak in Dali, China. PLoS Negl Trop Dis. 2009;3(9):e520.
6. Dorta-Contreras AJ, Padilla-Docal B, Moreira JM, Robles LM, Aroca JM, Alarcon F, Bu-Coifiu-Fanego R. Neuroimmunological findings of *Angiostrongylus cantonensis* meningitis in Ecuadorian patients. Arq Neuropsiquiatr. 2011;69(3):466-9.
7. Alicata JE. The discovery of *Angiostrongylus cantonensis* as a cause of human eosinophilic meningitis. Parasitol Today. 1991;7(6):151-3.
8. Lai CH, Yen CM, Chin C, Chung HC, Kuo HC, Lin HH. Eosinophilic meningitis caused by *Angiostrongylus cantonensis* after ingestion of raw frogs. Am J Trop Med Hyg. 2007;76(2):399-402.
9. Pino P, Taoufiq Z, Nitcheu J, Vouldoukis I, Mazier D. Blood-brain barrier breakdown during cerebral malaria: suicide or murder? Thromb Haemost. 2005;94(2):336-40.
10. Hu X, Li JH, Lan L, Wu FF, Zhang EP, Song ZM, Huang HC, Luo FJ, Pan CW, Tan F. In vitro study of the effects of *Angiostrongylus cantonensis* larvae extracts on apoptosis and dysfunction in the blood-brain barrier (BBB). PloS One. 2012;7(2):e32161.
11. Han YP, Li ZY, Li BC, Sun X, Zhu CC, Ling XT, Zheng HQ, Wu ZD, Lv ZY. Molecular cloning and characterization of a cathepsin B from *Angiostrongylus cantonensis*. Parasitol Res. 2011;109(2):369-78.
12. Ni F, Wang Y, Zhang J, Yu L, Fang W, Luo D. Cathepsin B-like and hemoglobin-type cysteine proteases: stage-specific gene expression in *Angiostrongylus cantonensis*. Exp Parasitol. 2012;131(4):433-41.
13. Toubarro D, Lucena-Robles M, Nascimento G, Santos R, Montiel R, Verissimo P, et al. Serine protease-mediated host invasion by the parasitic nematode *Steinernema carpocapsae*. J Biol Chem. 2010;285(40):30666-75.
14. Williamson AL, Lustigman S, Oksov Y, Deumic V, Plieskatt J, Mendez S, Zhan B, Bottazzi ME, Hotez PJ, Loukas A. Ancylostoma caninum MTP-1, an astacin-like metalloprotease secreted by infective hookworm larvae, is involved in tissue migration. Infect Immun. 2006;74(2):961-7.
15. McGonigle L, Mousley A, Marks NJ, Brennan GP, Dalton JP, Spithill TW, Day TA, Maule AG. The silencing of cysteine proteases in *Fasciola hepatica* newly excysted juveniles using

RNA interference reduces gut penetration. Int J Parasitol. 2008;38(2):149-55.
16. Chang SH, Tang P, Wang LC. A transcriptomic study on the pepsin-activated infective larvae of *Angiostrongylus cantonensis*. Mol Biochem Parasitol. 2011;179(1):47-50.
17. Lee JD, Yen CM. Protease secreted by the infective larvae of *Angiostrongylus cantonensis* and its role in the penetration of mouse intestine. Am J Trop Med Hyg. 2005;72(6):831-6.
18. Yu C, Wang Y, Zhang J, Fang W, Luo D. Immunolocalization and developmental expression patterns of two cathepsin B proteases (AC-cathB-1, -2) of *Angiostrongylus cantonensis*. Exp Parasitol. 2014;144C:27-33.
19. Li CK, Seth R, Gray T, Bayston R, Mahida YR, Wakelin D. Production of proinflammatory cytokines and inflammatory mediators in human intestinal epithelial cells after invasion by *Trichinella spiralis*. Infect Immun. 1998;66(5):2200-6.
20. Perry SW, Epstein LG, Gelbard HA. In situ trypan blue staining of monolayer cell cultures for permanent fixation and mounting. Biotechniques. 1997;22(6):1020-1, 4.
21. Stecker K, Koschel A, Wiedenmann B, Anders M. Loss of Coxsackie and adenovirus receptor downregulates alpha-catenin expression. Br J Cancer. 2009;101(9):1574-9.
22. Fuller E, Duckham C, Wood E. Disruption of epithelial tight junctions by yeast enhances the paracellular delivery of a model protein. Pharm Res. 2007;24(1):37-47.
23. Hansell E, Braschi S, Medzihradszky KF, Sajid M, Debnath M, Ingram J, et al. Proteomic analysis of skin invasion by blood fluke larvae. PLoS Negl Trop Dis. 2008;2(7):e262.
24. Butcher BA, Gagliardo LF, ManWarren T, Appleton JA. Larvae-induced plasma membrane wounds and glycoprotein deposition are insufficient for *Trichinella spiralis* invasion of epithelial cells. Mol Biochem Parasitol. 2000;107(2):207-18.
25. Gottstein B, Pozio E, Nockler K. Epidemiology, diagnosis, treatment, and control of trichinellosis. Clin Microbiol Rev. 2009;22(1):127-45.
26. Capo V, Despommier DD. Clinical aspects of infection with *Trichinella spp*. Clin Microbiol Rev. 1996;9(1):47-54.
27. Sawanyawisuth K. Treatment of angiostrongyliasis. Trans R Soc Trop Med Hyg. 2008;102(10):990-6.
28. Rodriguez R, Dequi RM, Peruzzo L, Mesquita PM, Garcia E, Fornari F. Abdominal angiostrongyliasis: report of two cases with different clinical presentations. Rev Inst Med Trop Sao Paulo. 2008;50(6):339-41.
29. Sawanyawisuth K, Pugkhem A, Mitchai J, Intapan PM, Anunnatsiri S, Limpawattana P P, Chotmongkol V. Abdominal angiostrongyliasis caused by *Angiostrongylus cantonensis*: a possible cause of eosinophilic infiltration in human digestive tract. Pathol Res Pract. 2010;206(2):102-4.
30. Peng H, Sun R, Zhang Q, Zhao J, Wei J, Zeng X, Zheng H, Wu Z. Interleukin 33 mediates type 2 immunity and inflammation in the central nervous system of mice infected with *Angiostrongylus cantonensis*. J Infect Dis. 2013;207(5):860-9.
31. Yu L, Wu X, Wei J, Liao Q, Xu L, Luo S, Zeng X, Zhao Y, Lv Z, Wu Z. Preliminary expression profile of cytokines in brain tissue of BALB/c mice with *Angiostrongylus cantonensis* infection. Parasit Vectors. 2015;8(1):328.
32. Drake L, Korchev Y, Bashford L, Djamgoz M, Wakelin D, Ashall F, et al. The major secreted product of the whipworm, *Trichuris*, is a pore-forming protein. Proc Biol Sci. 1994;257(1350):255-61.